Observation of structure in the J/ψ-pair mass spectrum

LHCb Collaboration ; Bernet, R ; Müller, K ; Owen, P ; Serra, N ; Steinkamp, O ; et al

DOI: https://doi.org/10.1016/j.scib.2020.08.032

Science Bulletin 65 (2020) 1983–1993

Contents lists available at ScienceDirect

Science Bulletin

journal homepage: www.elsevier.com/locate/scib

Science Bulletin
www.scibull.com

Article

Observation of structure in the J/ψ-pair mass spectrum

LHCb collaboration [1]

ARTICLE INFO

Article history:
Received 1 July 2020
Received in revised form 28 July 2020
Accepted 19 August 2020
Available online 29 August 2020

Keywords:
QCD
Exotics
Tetraquark
Spectroscopy
Quarkonium
Particle and resonance production

ABSTRACT

Using proton-proton collision data at centre-of-mass energies of $\sqrt{s} = 7, 8$ and 13 TeV recorded by the LHCb experiment at the Large Hadron Collider, corresponding to an integrated luminosity of 9 fb^{-1}, the invariant mass spectrum of J/ψ pairs is studied. A narrow structure around 6.9 GeV/c^2 matching the lineshape of a resonance and a broad structure just above twice the J/ψ mass are observed. The deviation of the data from nonresonant J/ψ-pair production is above five standard deviations in the mass region between 6.2 and 7.4 GeV/c^2, covering predicted masses of states composed of four charm quarks. The mass and natural width of the narrow $X(6900)$ structure are measured assuming a Breit-Wigner lineshape.

1. Introduction

The strong interaction is one of the fundamental forces of nature and it governs the dynamics of quarks and gluons. According to quantum chromodynamics (QCD), the theory describing the strong interaction, quarks are confined into hadrons, in agreement with experimental observations. The quark model [1,2] classifies hadrons into conventional mesons ($q\bar{q}$) and baryons (qqq or $\bar{q}\bar{q}\bar{q}$), and also allows for the existence of exotic hadrons such as tetraquarks ($qq\bar{q}\bar{q}$) and pentaquarks ($qqq\bar{q}\bar{q}$). Exotic states provide a unique environment to study the strong interaction and the confinement mechanism [3]. The first experimental evidence for an exotic hadron candidate was the $\chi_{c1}(3872)$ state observed in 2003 by the Belle collaboration [4]. Since then a series of novel states consistent with containing four quarks have been discovered [5]. Recently, the LHCb collaboration observed resonances interpreted to be pentaquark states [6–9]. All hadrons observed to date, including those of exotic nature, contain at most two heavy charm (c) or bottom (b) quarks, whereas many QCD-motivated phenomenological models also predict the existence of states consisting of four heavy quarks, i.e. $T_{Q_1Q_2\bar{Q}_3\bar{Q}_4}$, where Q_i is a c or a b quark [10–35]. Theoretically, the interpretation of the internal structure of such states usually assumes the formation of a Q_1Q_2 diquark and a $\bar{Q}_3\bar{Q}_4$ antidiquark attracting each other. Application of this diquark model successfully predicts the mass of the doubly charmed baryon Ξ_{cc}^{++} [36,37] and helps to explain the relative rates of bottom baryon decays [38].

Tetraquark states comprising only bottom quarks, $T_{bb\bar{b}\bar{b}}$, have been searched for by the LHCb and CMS collaborations in the $\Upsilon\mu^+\mu^-$ decay [39,40], with the Υ state consisting of a $b\bar{b}$ pair. However, the four-charm states, have not yet been studied in detail experimentally. A state could disintegrate into a pair of charmonium states such as J/ψ mesons, with each consisting of a $c\bar{c}$ pair. Decays to a J/ψ meson plus a heavier charmonium state, or two heavier charmonium states, with the heavier states decaying subsequently into a J/ψ meson and accompanying particles, are also possible. Predictions for the masses of states vary from 5.8 to 7.4 GeV/c^2 [10–26], which are above the masses of known charmonia and charmonium-like exotic states and below those of bottomonium hadrons. [2] This mass range guarantees a clean experimental environment to identify possible states in the J/ψ-pair (also referred to as di-J/ψ) invariant mass ($M_{\text{di-}J/\psi}$) spectrum.

In proton-proton (pp) collisions, a pair of J/ψ mesons can be produced in two separate interactions of gluons or quarks, named double-parton scattering (DPS) [41–43], or in a single interaction, named single-parton scattering (SPS) [44–51]. The SPS process includes both resonant production via intermediate states, which could be tetraquarks, and nonresonant production. Within the DPS process, the two J/ψ mesons are usually assumed to be produced independently, thus the distribution of any di-J/ψ observ-

[1] Authors are listed at the end of this paper.

[2] Energy units MeV = 10^6 eV, GeV = 10^9 eV and TeV = 10^{12} eV are used in this paper.

https://doi.org/10.1016/j.scib.2020.08.032
2095-9273/

able can be constructed using the kinematics from single J/ψ production. Evidence of DPS has been found in studies at the Large Hadron Collider (LHC) experiments [52–61] and the AFS experiment [62] in pp collisions, and at the Tevatron experiments [63–67] and the UA2 experiment [68] in proton-antiproton collisions. The LHCb experiment has measured the di-J/ψ production in pp collisions at centre-of-mass energies of $\sqrt{s} = 7$ [69] and 13 TeV [70]. The DPS contribution is found to dominate the high $M_{\text{di-}J/\psi}$ region, in agreement with expectation.

In this paper, fully charmed tetraquark states are searched for in the di-J/ψ invariant mass spectrum, using pp collision data collected by LHCb at $\sqrt{s} = 7, 8$ and 13 TeV, corresponding to an integrated luminosity of 9 fb^{-1}. The two J/ψ candidates in a pair are reconstructed through the $J/\psi \to \mu^+\mu^-$ decay, and are labelled randomly as either J/ψ_1 or J/ψ_2.

2. Detector and data set

The LHCb detector is designed to study particles containing b or c quarks at the LHC. It is a single-arm forward spectrometer covering the pseudorapidity range $2 < \eta < 5$, described in detail in Refs. [71,72]. The online event selection is performed by a trigger, which consists of a hardware stage, based on information from the calorimeter and muon systems, followed by a software stage, which applies a full event reconstruction. At the hardware stage, events are required to have at least one muon with high momentum transverse to the beamline, p_{T}. At the software stage, two oppositely charged muon candidates are required to have high p_{T} and to form a common vertex. Events are retained if there is at least one J/ψ candidate passing both the hardware and software trigger requirements. Imperfections in the description of the magnetic field and misalignment of subdetectors lead to a bias in the momentum measurement of charged particles, which is calibrated using reconstructed J/ψ and B^+ mesons [73], with well-known masses.

Simulated $J/\psi \to \mu^+\mu^-$ decays are used to study the signal properties, including the invariant mass resolution and the reconstruction efficiency. In the simulation, pp collisions are generated using PYTHIA [74] with a specific LHCb configuration [75]. Decays of unstable particles are described by EVTGEN [76], in which final-state radiation is generated using PHOTOS [77]. The interaction of the generated particles with the detector and its response are implemented using the GEANT4 toolkit [78], as described in Ref. [79].

3. Candidate selection

In the offline selection, two pairs of oppositely charged muon candidate tracks are reconstructed, with each pair forming a vertex of a J/ψ candidate. Each muon track must have $p_{\text{T}} > 0.65$ GeV/c and momentum $p > 6$ GeV/c. The J/ψ candidates are required to have a dimuon invariant mass in the range $3.0 < M_{\mu\mu} < 3.2$ GeV/c^2. A kinematic fit is performed for each J/ψ candidate constraining its vertex to coincide with a primary pp collision vertex (PV) [80]. The requirement of a good kinematic fit quality strongly suppresses the contamination of di-J/ψ candidates stemming from feed-down of b-hadrons, which decay at displaced vertices. The four muon tracks in a J/ψ-pair candidate are required to originate from the same PV, reducing to a negligible level the number of pile-up candidates with the two J/ψ candidates produced in separated pp collisions. Fake di-J/ψ candidates, comprising two muon-track candidates reconstructed from the same real particle, are rejected by requiring muons of the same charge to have trajectories separated by an angle inconsistent with zero. For events with more than one reconstructed di-J/ψ candidate, accounting for about 0.8% of the total sample, only one pair is randomly chosen.

The di-J/ψ signal yield is extracted by performing an extended unbinned maximum-likelihood fit to the two-dimensional distribution of J/ψ_1 and J/ψ_2 invariant masses, $\left(M^{(1)}_{\mu\mu}, M^{(2)}_{\mu\mu}\right)$, as displayed in Fig. 1, where projections of the data and the fit result are shown. For both J/ψ candidates, the signal mass shape is modelled by a Gaussian kernel with power-law tails [81]. Each component of combinatorial background, consisting of random combinations of muon tracks, is described by an exponential function. The total di-J/ψ signal yield is measured to be $(33.57 \pm 0.23) \times 10^3$, where the uncertainty is statistical.

The di-J/ψ transverse momentum ($p_{\text{T}}^{\text{di-}J/\psi}$) in SPS production is expected to be, on average, higher than that in DPS [50]. The high-$p_{\text{T}}^{\text{di-}J/\psi}$ region is thus exploited to select a data sample with enhanced SPS production, which could include contributions from states. Two different approaches are applied. In the first approach (denoted as $p_{\text{T}}^{\text{di-}J/\psi}$-threshold), J/ψ-pair candidates are selected with the requirement $p_{\text{T}}^{\text{di-}J/\psi} > 5.2$ GeV/c, which maximises the statistical significance of the SPS signal yield, $N_{\text{SPS}}/\sqrt{N_{\text{total}}}$. N_{SPS} and N_{total} are yields of the SPS component and total di-J/ψ candidates in the $M_{\text{di-}J/\psi}$ range between 6.2 and 7.4 GeV/c^2, respectively. This mass region covers the predicted masses of states decaying into a J/ψ pair. In the second approach (denoted as $p_{\text{T}}^{\text{di-}J/\psi}$-binned), di-$J/\psi$ candidates are categorised into six $p_{\text{T}}^{\text{di-}J/\psi}$ intervals with boundaries $\{0, 5, 6, 8, 9.5, 12, 50\}$ GeV/c, defined to obtain equally populated bins of SPS signal events in the $6.2 < M_{\text{di-}J/\psi} < 7.4$ GeV/c^2 range. For both scenarios, the DPS yield in the signal region is extrapolated from the high-$M_{\text{di-}J/\psi}$ region using the wide-range distribution constructed from available double-differential J/ψ cross-sections [82–84] as performed in Ref. [70]. The high-$M_{\text{di-}J/\psi}$ region is chosen so that the SPS yield is negligible compared to DPS. The SPS yield is obtained by subtracting the DPS contribution from the total number of J/ψ-pair signals.

The $M_{\text{di-}J/\psi}$ distribution for candidates with $p_{\text{T}}^{\text{di-}J/\psi} > 5.2$ GeV/c and $3.065 < M^{(1),(2)}_{\mu\mu} < 3.135$ GeV/c^2 is shown in Fig. 2. The di-J/ψ mass is calculated by constraining the reconstructed mass of each J/ψ candidate to its known value [85]. The spectrum shows a broad structure just above twice the J/ψ mass threshold ranging from 6.2 to 6.8 GeV/c^2 (dubbed threshold enhancement in the following) and a narrower structure at about 6.9 GeV/c^2, referred to hereafter as $X(6900)$. There is also a hint of another structure around 7.2 GeV/c^2, whereas there are no evident structures at higher invariant mass. Several cross-checks are performed to investigate the origin of these structures and to exclude that they are experimental artifacts. The threshold enhancement and the $X(6900)$ structure become more pronounced in higher $p_{\text{T}}^{\text{di-}J/\psi}$ intervals, and they are present in subsamples split according to different beam or detector configurations for data collection. The structures are not caused by the experimental efficiency, since the efficiency variation across the whole $M_{\text{di-}J/\psi}$ range is found to be marginal. Residual background, in which a muon track is reused or at least one J/ψ candidate is produced from a b-hadron decay, is observed to have no structure. The possible contribution of J/ψ pairs from Υ decays is estimated to be negligible and distributed uniformly in the $M_{\text{di-}J/\psi}$ distribution. In Fig. 2, the $M_{\text{di-}J/\psi}$ distribution for background pairs with $M^{(1),(2)}_{\mu\mu}$ in the range 3.00—3.05 GeV/c^2 or 3.15—3.20 GeV/c^2 is also shown, with the yield normalised by interpolating the background into the J/ψ signal region, which accounts for around 15% of the total candidates. There is no evidence of structures in the $M_{\text{di-}J/\psi}$ distribution of background candidates.

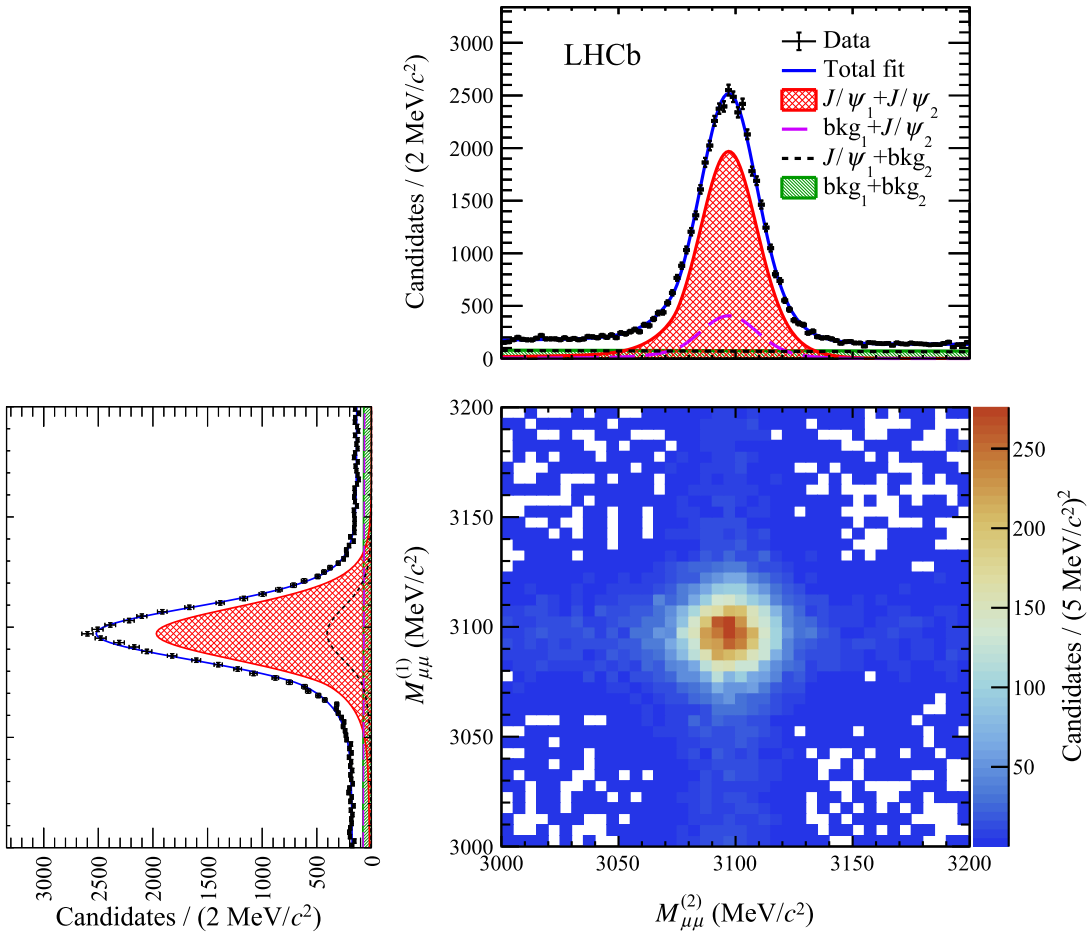

Fig. 1. (Bottom right) Two-dimensional $\left(M^{(1)}_{\mu\mu}, M^{(2)}_{\mu\mu}\right)$ distribution of di-J/ψ candidates and its projections on (bottom left) $M^{(1)}_{\mu\mu}$ and (top) $M^{(2)}_{\mu\mu}$. Four components are present as each projection consists of signal and background J/ψ candidates. The labels $J/\psi_{1,2}$ and $\mathrm{bkg}_{1,2}$ represent the signal and background contributions, respectively, in the $M^{(1),(2)}_{\mu\mu}$ distribution.

4. Investigation of the J/ψ-pair invariant mass spectrum

To remove background pairs that have at least one background J/ψ candidate, the *sPlot* weighting method [86] is applied, where the weights are calculated from the fit to the two-dimensional $\left(M^{(1)}_{\mu\mu}, M^{(2)}_{\mu\mu}\right)$ distribution. The background-subtracted di-J/ψ spectra in the range $6.2 < M_{\text{di-J}/\psi} < 9.0\ \text{GeV}/c^2$ are shown in Fig. 3 for candidates with $p_{\mathrm{T}}^{\text{di-J}/\psi} > 5.2\ \text{GeV}/c$ and Fig. 4 for candidates in the six $p_{\mathrm{T}}^{\text{di-J}/\psi}$ intervals, which are investigated by weighted unbinned maximum-likelihood fits [87]. The $M_{\text{di-J}/\psi}$ distribution of signal events is expected to be dominated by the sum of the non-resonant SPS (NRSPS) and DPS production, which have smooth shapes (referred to as continuum in the following). The DPS continuum is described by a two-body phase-space function multiplied by the product of an exponential function and a second order polynomial function, whose parameters are fixed according to the $M_{\text{di-J}/\psi}$ distribution constructed from J/ψ differential cross-sections. Its yield is determined by extrapolation from the $M_{\text{di-J}/\psi} > 12\ \text{GeV}/c^2$ region, which is dominated and well described by the DPS distribution. The continuum NRSPS is modelled by a two-body phase-space distribution multiplied by an exponential function determined from the data. The combination of continuum NRSPS and DPS does not provide a good description of the data, as is illustrated in Fig. 3a. The $M_{\text{di-J}/\psi}$ spectrum in the data is tested against the hypothesis that only NRSPS and DPS components are present in the range $6.2 < M_{\text{di-J}/\psi} < 7.4\ \text{GeV}/c^2$ (null hypothesis) using a χ^2 test statistic. Pseudoexperiments are generated and fitted according to the null hypothesis, and the fraction of these fits with a χ^2 value exceeding that in the data is converted into a sig-

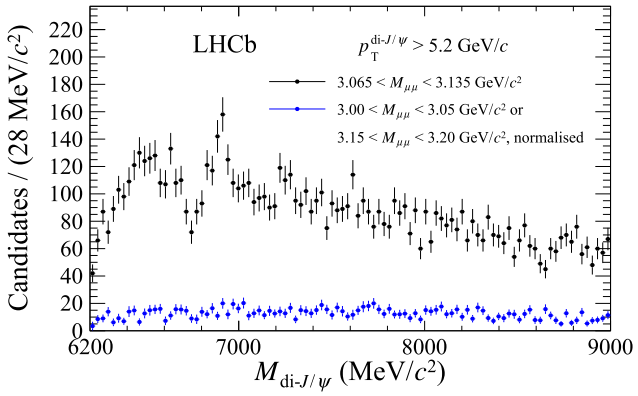

Fig. 2. Invariant mass spectrum of J/ψ-pair candidates passing the $p_{\mathrm{T}}^{\text{di-J}/\psi} > 5.2\ \text{GeV}/c$ requirement with reconstructed J/ψ masses in the (black) signal and (blue) background regions, respectively.

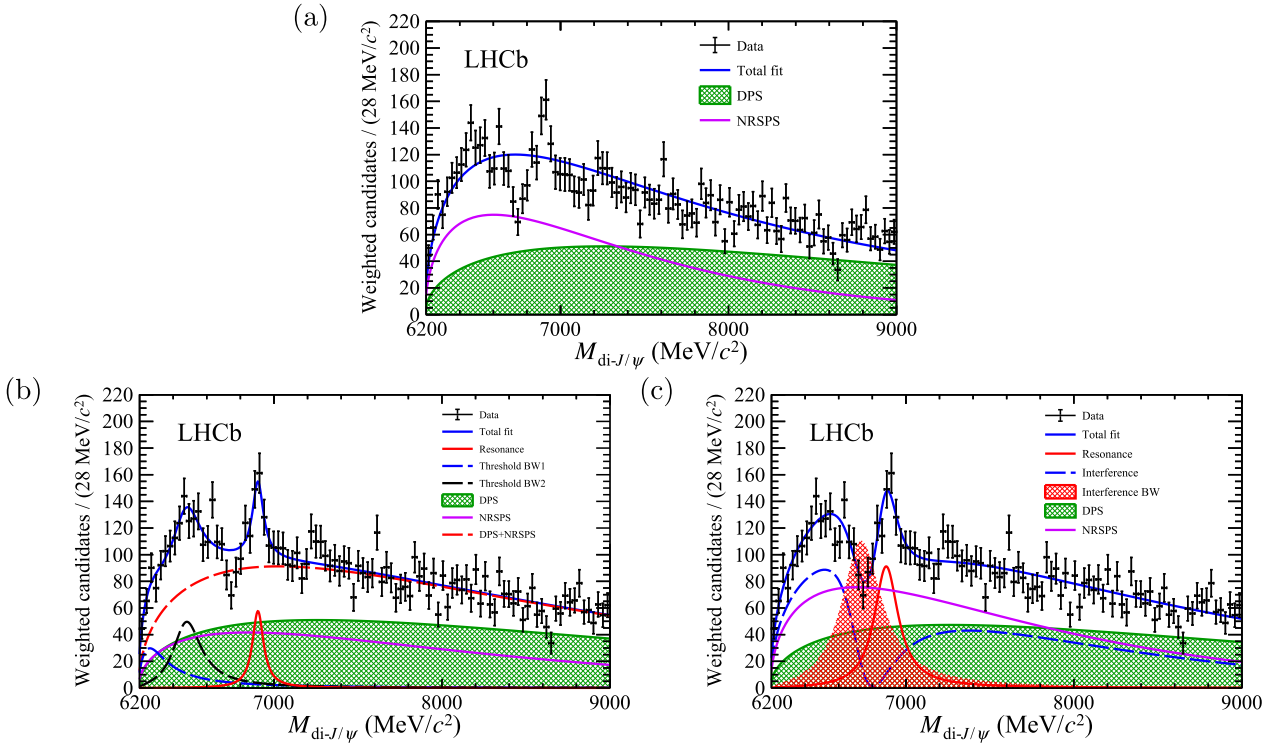

Fig. 3. Invariant mass spectra of weighted di-J/ψ candidates with $p_{\mathrm{T}}^{\text{di-}J/\psi} > 5.2$ GeV/c and overlaid projections of the $p_{\mathrm{T}}^{\text{di-}J/\psi}$-threshold fit using (a) the NRSPS plus DPS model, (b) model I, and (c) model II.

nificance. Considering the sample in the $p_{\mathrm{T}}^{\text{di-}J/\psi} > 5.2$ GeV/c region, the null hypothesis is inconsistent with the data at 3.4 standard deviations (σ). A test performed simultaneously in the aforementioned six $p_{\mathrm{T}}^{\text{di-}J/\psi}$ regions yields a discrepancy of 6.0σ with the null hypothesis. A higher value is obtained in the latter case attributed to the presence of the structure at the same $M_{\text{di-}J/\psi}$ location in different $p_{\mathrm{T}}^{\text{di-}J/\psi}$ intervals. A cross-check is performed by dividing the data into five or seven $p_{\mathrm{T}}^{\text{di-}J/\psi}$ regions instead, which results in significance values consistent with the nominal 6.0σ. The significance values are summarised in Table 1 (any structure beyond NRSPS plus DPS).

The structures in the $M_{\text{di-}J/\psi}$ distribution can have various interpretations. There may be one or more resonant states decaying directly into a pair of J/ψ mesons, or states decaying into a pair of J/ψ mesons through feed-down of heavier quarkonia, for example $T_{cc\bar{c}\bar{c}} \to \chi_c(\to J/\psi\gamma)J/\psi$ where the photon escapes detection. In the latter case, such a state would be expected to peak at a lower $M_{\text{di-}J/\psi}$ position, close to the di-J/ψ mass threshold, and its structure would be broader compared to that from a direct decay. This feed-down is unlikely an explanation for the narrow $X(6900)$ structure. Rescattering of two charmonium states produced by SPS close to their mass threshold may also generate a narrow structure [88–91]. The two thresholds close to the $X(6900)$ structure could be formed by $\chi_{c0}\chi_{c0}$ pairs at 6829.4 MeV/c^2 and $\chi_{c1}\chi_{c0}$ pairs at 6925.4 MeV/c^2, respectively. Whereas a resonance is often described by a relativistic Breit-Wigner (BW) function [85], the lineshape of a structure with rescattering effects taken into account is more complex. In principle, resonant production can interfere with NRSPS of the same spin-parity quantum numbers (J^{PC}), resulting in a coherent sum of the two components and thus a modification of the total $M_{\text{di-}J/\psi}$ distribution.

Two different models of the structure lineshape providing a reasonable description of the data are investigated. The $X(6900)$ lineshape parameters and yields are derived from fits to the $p_{\mathrm{T}}^{\text{di-}J/\psi}$-threshold sample. Simultaneous $p_{\mathrm{T}}^{\text{di-}J/\psi}$-binned fits are also performed as a cross-check and the variation of lineshape parameters is considered as a source of systematic uncertainties. Due to its low significance, the structure around 7.2 GeV/c^2 has been neglected.

In model I, the $X(6900)$ structure is considered as a resonance, whereas the threshold enhancement is described through a superposition of two resonances. The lineshapes of these resonances are described by S-wave relativistic BW functions multiplied by a two-body phase-space distribution. The experimental resolution on $M_{\text{di-}J/\psi}$ is below 5 MeV/c^2 over the full mass range and negligible compared to the widths of the structures. The projections of the $p_{\mathrm{T}}^{\text{di-}J/\psi}$-threshold fit using this model are shown in Fig. 3b. The mass, natural width and yield are determined to be $m[X(6900)] = 6905 \pm 11$ MeV/c^2, $\Gamma[X(6900)] = 80 \pm 19$ MeV and $N_{\text{sig}} = 252 \pm 63$, where biases on the statistical uncertainties have been corrected using a bootstrap method [92]. The goodness of fit is studied using a χ^2 test statistic and found to be $\chi^2/\text{ndof} = 112.7/89$, corresponding to a probability of 4.6%. The fit is also performed assuming the threshold enhancement as due to a single wide resonance (see the Supplementary materials); the fit quality is found significantly poorer and thus this model is not further investigated.

A comparison between the best fit result of model I and the data reveals a tension around 6.75 GeV/c^2, where the data shows a dip. In an attempt to describe the dip, model II allows for interference between the NRSPS component and a resonance for the threshold enhancement. The coherent sum of the two components is defined as

$$\left| A e^{i\phi} \sqrt{f_{\text{nr}}(M_{\text{di-}J/\psi})} + \text{BW}(M_{\text{di-}J/\psi}) \right|^2, \quad (1)$$

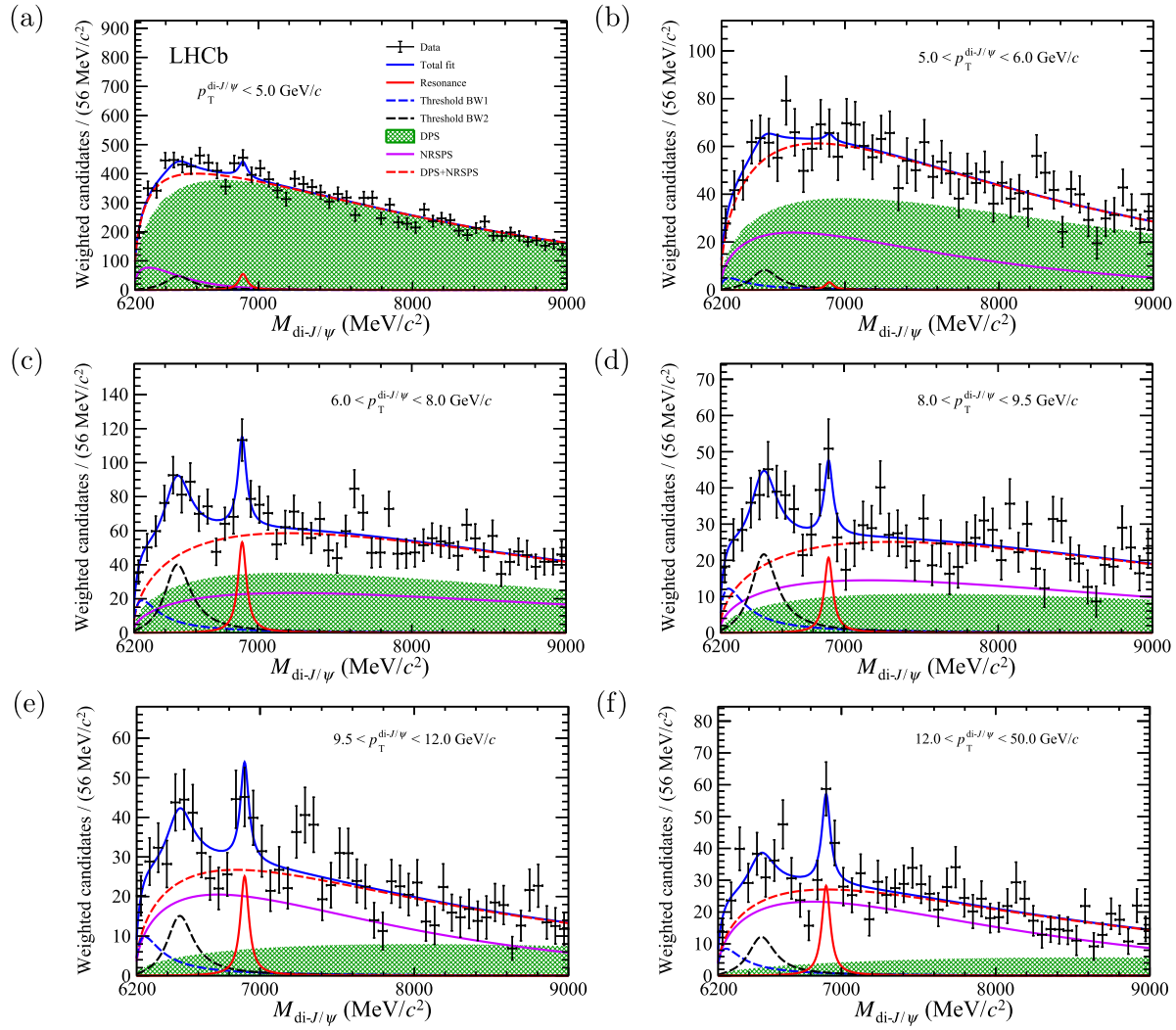

Fig. 4. Invariant mass spectra of weighted di-J/ψ candidates in bins of $p_T^{di\text{-}J/\psi}$ and overlaid projections of the $p_T^{di\text{-}J/\psi}$-binned fit with model I.

Table 1
Global significance evaluated under the various assumptions described in the text.

Structure	Significance	
	$p_T^{di\text{-}J/\psi}$-threshold	$p_T^{di\text{-}J/\psi}$-binned
Any structure beyond NRSPS plus DPS	3.4σ	6.0σ
Threshold enhancement plus $X(6900)$	6.4σ	6.9σ
Threshold enhancement	6.0σ	6.5σ
$X(6900)$	5.1σ	5.4σ

where A and ϕ are the magnitude and phase of the nonresonant component, relative to the BW lineshape for the resonance, assumed to be independent of $M_{di\text{-}J/\psi}$, and $f_{nr}(M_{di\text{-}J/\psi})$ is an exponential function. The interference term in Eq. (1) is then added incoherently to the BW function describing the $X(6900)$ structure and the DPS description. The fit to the $p_T^{di\text{-}J/\psi}$-threshold sample with this model has a probability of 15.5% (χ^2/ndf = 104.7/91), and its projections are illustrated in Fig. 3c. In this case, the mass, natural width and yield are determined to be $m[X(6900)] = 6886 \pm 11$ MeV/c^2, $\Gamma[X(6900)] = 168 \pm 33$ MeV and $N_{sig} = 784 \pm 148$. A larger $X(6900)$ width and yield are preferred in comparison to model I. Here it is assumed that the whole NRSPS production is involved in the interference with the lower-mass resonance despite that there may be several components with different quantum numbers in the NRSPS and more than one resonance in the threshold enhancement.

Fits to the $M_{di\text{-}J/\psi}$ distributions in the six individual $p_T^{di\text{-}J/\psi}$ bins are shown in Fig. 4 for model I, while those for model II are given in the Supplementary materials. An additional model describing the dip and the $X(6900)$ structure simultaneously by using the interference between the NRSPS and a BW resonance around 6.9 GeV/c^2 is also considered, however the fit quality is clearly poorer, as illustrated in the Supplementary materials. Alternative lineshapes, other than the BW, may also be possible to describe these structures and will be the subject of future studies.

The increase of the likelihood between the fits with or without considering the $X(6900)$ and the threshold enhancement structures on top of the continuum NRSPS plus DPS model is taken as the test statistic to calculate the combined global significance of the two structures [93] in the $6.2 < M_{di\text{-}J/\psi} < 7.4$ GeV/c^2 region, where pseudoexperiments are also generated to evaluate the significance. Only model I is studied, where the interference between the NRSPS and the threshold enhancement is not included. Similarly, the significance for either the threshold enhancement or the $X(6900)$ structure is evaluated assuming the presence of the other along with the NRSPS and DPS continuum. The significance is determined from both $p_T^{di\text{-}J/\psi}$-threshold and $p_T^{di\text{-}J/\psi}$-binned fits, and summarised in

Table 2
Systematic uncertainties on the mass (m) and natural width (Γ) of the $X(6900)$ structure.

Component	Without interference		With interference	
	m (MeV/c^2)	Γ (MeV)	m (MeV/c^2)	Γ (MeV)
sPlot weights	0.8	10.3	4.4	36.9
Experimental resolution	0.0	1.4	0.0	0.6
NRSPS + DPS modelling	0.8	16.1	3.5	9.3
$X(6900)$ shape	0.0	0.3	0.4	0.2
Dependence on $p_{\mathrm{T}}^{\text{di-J/}\psi}$	4.6	13.5	6.2	56.7
b-hadron feed-down	0.0	0.2	0.0	5.3
Structure at 7.2 GeV/c^2	1.3	9.2	6.7	5.2
Threshold structure shape	5.2	20.5	–	–
NRSPS phase	–	–	0.3	1.3
Total	7	33	11	69

Table 1. The results are above 5σ for the two structures, with slightly higher significance for the $p_{\mathrm{T}}^{\text{di-J/}\psi}$-binned case.

Systematic uncertainties on the measurements of the mass and natural width of the $X(6900)$ structure are reported in Table 2. They include variations of the results obtained by: including an explicit component in the $M_{\text{di-J/}\psi}$ fits for the J/ψ combinatorial background rather than subtracting it using the weighting method (*sPlot* weights in Table 2); convolving the $M_{\text{di-J/}\psi}$ fit functions with a Gaussian function of 5 MeV/c^2 width to account for the invariant mass resolution (Experimental resolution); using alternative functions to describe the NRSPS component and varying the DPS yield (NRSPS plus DPS modelling); using an alternative P-wave BW function for the $X(6900)$ structure and varying the hadron radius in the BW function from 2 to 5 GeV^{-1} ($X(6900)$ shape); obtaining results from a simultaneous fit to the $M_{\text{di-J/}\psi}$ distributions in the six $p_{\mathrm{T}}^{\text{di-J/}\psi}$ bins which covers the uncertainty due to variations of the NRSPS, DPS shapes and the NRSPS-resonance interference with respect to $p_{\mathrm{T}}^{\text{di-J/}\psi}$ (Dependence on $p_{\mathrm{T}}^{\text{di-J/}\psi}$); including an explicit contribution for J/ψ mesons from b-hadron feed-down (b-hadron feed-down) or adding a BW component for the 7.2 GeV/c^2 structure (Structure at 7.2 GeV/c^2); modelling the threshold structure using an alternative Gaussian function with asymmetric power-law tails, or fitting in a reduced $M_{\text{di-J/}\psi}$ range excluding the threshold structure (Threshold structure shape); allowing the relative phase in the NRSPS component to vary linearly with $M_{\text{di-J/}\psi}$ (NRSPS phase). The total uncertainties are determined to be 7 MeV/c^2 and 33 MeV for the mass and natural width, respectively, without considering any interference, and 11 MeV/c^2 and 69 MeV when the interference between NRSPS and the threshold structure is introduced.

For the scenario without interference, the production cross-section of the $X(6900)$ structure relative to that of all J/ψ pairs (inclusive), times the branching fraction $\mathscr{B}(X(6900)\to J/\psi J/\psi)$, $\mathscr{R}$, is determined in the pp collision data at $\sqrt{s}=13$ TeV. The measurement is obtained for both J/ψ mesons in the fiducial region of transverse momentum below 10 GeV/c and rapidity between 2.0 and 4.5. An event-by-event efficiency correction is performed to obtain the signal yield at production. The residual contamination from b-hadron feed-down is subtracted from inclusive J/ψ-pair production following Ref. [84]. The systematic uncertainties on the $X(6900)$ yield are estimated in a similar way to that for the mass and natural width, while other systematic uncertainties mostly cancel in the ratio. The production ratio is measured to be $\mathscr{R}=[1.1\pm0.4(\mathrm{stat})\pm0.3(\mathrm{syst})]\%$ without any $p_{\mathrm{T}}^{\text{di-J/}\psi}$ requirement and $\mathscr{R}=[2.6\pm0.6(\mathrm{stat})\pm0.8(\mathrm{syst})]\%$ for $p_{\mathrm{T}}^{\text{di-J/}\psi}>5.2$ GeV/c.

5. Summary

In conclusion, using pp collision data at centre-of-mass energies of 7, 8 and 13 TeV collected with the LHCb detector, corresponding to an integrated luminosity of 9 fb^{-1}, the J/ψ-pair invariant mass spectrum is studied. The data in the mass range between 6.2 and 7.4 GeV/c^2 are found to be inconsistent with the hypothesis of NRSPS plus DPS continuum. A narrow structure, $X(6900)$, matching the lineshape of a resonance and a broad structure next to the di-J/ψ mass threshold are found. The global significance of either the broad or the $X(6900)$ structure is determined to be larger than five standard deviations. Describing the $X(6900)$ structure with a Breit-Wigner lineshape, its mass and natural width are determined to be

$$m[X(6900)]=6905\pm11\pm7\ \mathrm{MeV}/c^2, \tag{2}$$

and

$$\Gamma[X(6900)]=80\pm19\pm33\ \mathrm{MeV}, \tag{3}$$

assuming no interference with the NRSPS continuum is present, where the first uncertainty is statistical and the second systematic. When assuming the NRSPS continuum interferes with the broad structure close to the di-J/ψ mass threshold, they become

$$m[X(6900)]=6886\pm11\pm11\ \mathrm{MeV}/c^2 \tag{4}$$

and

$$\Gamma[X(6900)]=168\pm33\pm69\ \mathrm{MeV}. \tag{5}$$

The $X(6900)$ structure could originate from a hadron state consisting of four charm quarks, predicted in various tetraquark models. The broad structure close to the di-J/ψ mass threshold could be due to a mixture of multiple four-charm quark states or have contributions from feed-down decays of four-charm states through heavier quarkonia. Other interpretations cannot presently be ruled out, for example the rescattering of two charmonium states produced close to their mass threshold. More data along with additional measurements, including determination of the spin-parity quantum numbers and p_{T} dependence of the production cross-section, are needed to provide further information about the nature of the observed structure.

Conflict of interest

The authors declare that they have no conflict of interest.

Acknowledgments

We express our gratitude to our colleagues in the CERN accelerator departments for the excellent performance of the LHC. We thank the technical and administrative staff at the LHCb institutes. We acknowledge support from CERN and from the national agencies: CAPES, CNPq, FAPERJ and FINEP (Brazil); MOST and NSFC (China); CNRS/IN2P3 (France); BMBF, DFG and MPG (Germany); INFN (Italy); NWO (Netherlands); MNiSW and NCN (Poland); MEN/IFA (Romania); MSHE (Russia); MinECo (Spain); SNSF and

SER (Switzerland); NASU (Ukraine); STFC (United Kingdom); DOE NP and NSF (USA). We acknowledge the computing resources that are provided by CERN, IN2P3 (France), KIT and DESY (Germany), INFN (Italy), SURF (Netherlands), PIC (Spain), GridPP (United Kingdom), RRCKI and Yandex LLC (Russia), CSCS (Switzerland), IFIN-HH (Romania), CBPF (Brazil), PL-GRID (Poland) and OSC (USA). We are indebted to the communities behind the multiple open-source software packages on which we depend. Individual groups or members have received support from AvH Foundation (Germany); EPLANET, Marie Skłodowska-Curie Actions and ERC (European Union); A*MIDEX, ANR, Labex P2IO and OCEVU, and Région Auvergne-Rhône-Alpes (France); Key Research Program of Frontier Sciences of CAS, CAS PIFI, and the Thousand Talents Program (China); RFBR, RSF and Yandex LLC (Russia); GVA, XuntaGal and GENCAT (Spain); the Royal Society and the Leverhulme Trust (United Kingdom).

Appendix A. Supplementary materials

Supplementary materials to this article can be found online at https://doi.org/10.1016/j.scib.2020.08.032.

References

[1] Gell-Mann M. A schematic model of baryons and mesons. Phys Lett 1964;8:214.
[2] Zweig G. An SU_3 model for strong interaction symmetry and its breaking. Version 1, Tech. Rep. CERN-TH-401, CERN, Geneva; 1964.
[3] Brambilla N, Eidelman S, Foka P, et al. QCD and strongly coupled gauge theories: challenges and perspectives. Eur Phys J C 2014;74:2981.
[4] Belle Collaboration, Choi SK, et al. Observation of a narrow charmonium-like state in exclusive $B^{\pm}K^{\pm}\pi^{+}\pi^{-}J/\psi$ decays. Phys Rev Lett 91; 2003:262001.
[5] Olsen SL, Skwarnicki T, Zieminska D. Nonstandard heavy mesons and baryons: experimental evidence. Rev Mod Phys 2018;90:015003.
[6] LHCb Collaboration, Aaij R, et al. Observation of J/ψ resonances consistent with pentaquark states in $\Lambda_b^0 J/\psi K^-$ decays. Phys Rev Lett 115;2015:072001.
[7] LHCb Collaboration, Aaij R, et al. Model-independent evidence for J/ψ contributions to $\Lambda_b^0 J/\psi K^-$ decays. Phys Rev Lett 2016;117:082002.
[8] LHCb Collaboration, Aaij R, et al. Evidence for exotic hadron contributions to $\Lambda_b^0 J/\psi\pi^-$ decays. Phys Rev Lett 2016;117:082003.
[9] LHCb Collaboration, Aaij R, et al. Observation of a narrow $P_c(4312)^+$ state, and of two-peak structure of the $P_c(4450)^+$. Phys Rev Lett 122;2019:222001.
[10] Iwasaki Y. Is a state $c\bar{c}c\bar{c}$ found at 6.0 GeV? Phys Rev Lett 1976;36:1266.
[11] Chao K-T. The $(cc)-(\bar{c}\bar{c})$ (diquark-antidiquark) states in e^+e^- annihilation. Z Phys C 1981;7:317.
[12] Ader J-P, Richard J-M, Taxil P. Do narrow heavy multiquark states exist? Phys Rev D 1982;25:2370.
[13] Li B-A, Liu K-F. J/ψ pair production in hadronic collisions. Phys Rev D 1984;29:426.
[14] Badalian AM, Ioffe BL, Smilga AV. Four quark states in heavy quark systems. Nucl Phys 1987;281:B85.
[15] Berezhnoy AV, Luchinsky AV, Novoselov AA. Heavy tetraquarks production at the LHC. Phys Rev D 2012;86:034004.
[16] Wu J, Liu Y-R, Chen K, et al. Heavy-flavored tetraquark states with the $QQ\bar{Q}\bar{Q}$ configuration. Phys Rev D 2018;97:094015.
[17] Karliner M, Nussinov S, Rosner JL. $QQ\bar{Q}\bar{Q}$ states: masses, production, and decays. Phys Rev D 2017;95:034011.
[18] Barnea N, Vijande J, Valcarce A. Four-quark spectroscopy within the hyperspherical formalism. Phys Rev D 2006;73:054004.
[19] Debastiani VR, Navarra FS. A non-relativistic model for the $[cc][\bar{c}\bar{c}]$ tetraquark. Chin Phys C 2019;43:013105.
[20] Liu M-S, L Q-F, Zhong X-H, et al. All-heavy tetraquarks. Phys Rev 2019;100:016006.
[21] Chen W, Chen H-X, Liu X, et al. Hunting for exotic doubly hidden-charm/bottom tetraquark states. Phys Lett B 2017;773:247.
[22] Wang G-J, Meng L, Zhu S-L. Spectrum of the fully-heavy tetraquark state $QQ\bar{Q}'\bar{Q}'$. Phys Rev D 2019;100:096013.
[23] Bedolla MA, Ferretti J, Roberts CD, et al. Spectrum of fully-heavy tetraquarks from a diquark+antidiquark perspective. arXiv:1911.00960, 2019.
[24] Lloyd RJ, Vary JP. All-charm tetraquarks. Phys Rev D 2004;70:014009.
[25] Chen X. Fully-charm tetraquarks: $cc\bar{c}\bar{c}$. arXiv:2001.06755, 2020.
[26] Wang Z-G, Di Z-Y. Analysis of the vector and axialvector $QQ\bar{Q}\bar{Q}$ tetraquark states with QCD sum rules. Acta Phys Polon B 2019;50:1335.
[27] Anwar MN, Ferretti J, Guo F-K, et al. Spectroscopy and decays of the fully-heavy tetraquarks. Eur Phys J C 2018;78:647.
[28] Liu Y-R, Chen H-X, Chen W, et al. Pentaquark and tetraquark states. Prog Part Nucl Phys 2019;107:237.
[29] Esposito A, Polosa AD. A $bb\bar{b}\bar{b}$ di-bottomonium at the LHC? Eur Phys J C 2018;78:782.
[30] Becchi C, Giachino A, Maiani L, et al. Search for $bb\bar{b}\bar{b}$ tetraquark decays in 4 muons, B^+B^-, $B^0\bar{B}^0$ and $B_s^0\bar{B}_s^0$ channels at LHC. Phys Lett B 2020;806:135495.
[31] Bai Y, Lu S, Osborne J. Beauty-full tetraquarks. Phys Lett B 2019;798:134930.
[32] Richard J-M, Valcarce A, Vijande J. String dynamics and metastability of all-heavy tetraquarks. Phys Rev D 2017;95:054019.
[33] Chen Y, Vega-Morales R. Golden probe of the di-Υ threshold. arXiv:1710.02738, 2017.
[34] Chen X. Fully-heavy tetraquarks: $bb\bar{c}\bar{c}$ and $bc\bar{b}\bar{c}$. Phys Rev D 2019;100:094009.
[35] Berezhnoy AV, Likhoded AK, Novoselov AA. Υ-meson pair production at LHC. Phys Rev D 2013;87:054023.
[36] Karliner M, Rosner JL. Baryons with two heavy quarks: masses, production, decays, and detection. Phys Rev D 2014;90:094007.
[37] LHCb Collaboration, Aaij R, et al. Observation of the doubly charmed baryon Ξ_{cc}^{++}. Phys Rev Lett 2017;119:112001.
[38] LHCb Collaboration, Aaij R, et al. Isospin amplitudes in $\Lambda_b^0 \to J/\psi\Lambda(\Sigma^0)$ and $\Xi_b^0 \to J/\psi\Xi^0(\Lambda)$ decays. Phys Rev Lett 2020;124:111802.
[39] LHCb Collaboration, Aaij R, et al. Search for beautiful tetraquarks in the $\Upsilon(1S)\mu^+\mu^-$ invariant-mass spectrum. J High Energy Phys 2018;10:086.
[40] CMS Collaboration, Sirunyan AM, et al. Measurement of the $\Upsilon(1S)$ pair production cross section and search for resonances decaying to $\Upsilon(1S)\mu^+\mu^-$ in proton-proton collisions at $\sqrt{s}$ = 13 TeV. arXiv:2002.06393, 2020.
[41] Calucci G, Treleani D. Minijets and the two-body parton correlation. Phys Rev D 1998;57:503.
[42] Calucci G, Treleani D. Proton structure in transverse space and the effective cross section. Phys Rev D 1999;60:054023.
[43] Del Fabbro A, Treleani D. Scale factor in double parton collisions and parton densities in transverse space. Phys Rev D 2001;63:057901.
[44] Sun L-P, Han H, Chao K-T. Impact of J/ψ pair production at the LHC and predictions in nonrelativistic QCD. Phys Rev D 2016;94:074033.
[45] Likhoded AK, Luchinsky AV, Poslavsky SV. Production of $J/\psi+\chi_c$ and $J/\psi+J/\psi$ with real gluon emission at LHC. Phys Rev D 2016;94:054017.
[46] Shao H-S. HELAC-Onia: an automatic matrix element generator for heavy quarkonium physics. Comput Phys Commun 2013;184:2562.
[47] Shao H-S. HELAC-Onia 2.0: an upgraded matrix-element and event generator for heavy quarkonium physics. Comput Phys Commun 2016;198:238.
[48] Baranov SP. Pair production of J/ψ mesons in the k_t-factorization approach. Phys Rev D 2011;84:054012.
[49] Lansberg J-P, Shao H-S. Production of $J/\psi+\eta_c$ versus $J/\psi+J/\psi$ at the LHC: Importance of real α_s^5 corrections. Phys Rev Lett 2013;111:122001.
[50] Lansberg J-P, Shao H-S. J/ψ-pair production at large momenta: indications for double parton scatterings and large α_s^5 contributions. Phys Lett B 2015;751:479.
[51] Lansberg J-P, Shao H-S. Double-quarkonium production at a fixed-target experiment at the LHC (AFTER@LHC). Nucl Phys B 2015;900:273.
[52] CMS Collaboration, Chatrchyan S, et al. Study of double parton scattering using W + 2-jet events in proton-proton collisions at $\sqrt{s}=7$ TeV. J High Energy Phys 2014;03:032.
[53] CMS Collaboration, Khachatryan V, et al. Measurement of prompt J/ψ pair production in pp collisions at $\sqrt{s}$ = 7 TeV. J High Energy Phys 2014;09:094.
[54] CMS Collaboration, Khachatryan V, et al. Observation of $\Upsilon(1S)$ pair production in proton-proton collisions at $\sqrt{s}$ = 8 TeV. arXiv:1610.07095, 2016.
[55] ATLAS Collaboration, Aad G, et al. Measurement of the production of a W boson in association with a charm quark in pp collisions at $\sqrt{s}=7$ TeV with the ATLAS detector. J High Energy Phys 2014;05:068.
[56] ATLAS Collaboration, Aad G, et al. Observation and measurements of the production of prompt and non-prompt J/ψ mesons in association with a Z boson in pp collisions at $\sqrt{s}$ = 8 TeV with the ATLAS detector. Eur Phys J C 2015;75:229.
[57] ATLAS Collaboration, Aaboud M, et al. Study of hard double-parton scattering in four-jet events in pp collisions at $\sqrt{s}=7$ TeV with the ATLAS experiment. J High Energy Phys 2016;11:110.
[58] ATLAS Collaboration, Aaboud M, et al. Measurement of the prompt J/ψ pair production cross-section in pp collisions at $\sqrt{s}$ = 8 TeV with the ATLAS detector. Eur Phys J C 2017;77:76.
[59] LHCb Collaboration, Aaij R, et al. Observation of double charm production involving open charm in collisions at $\sqrt{s}$=7 TeV. J High Energy Phys 2012;06:141. Addendum ibid. 2014;03:108.
[60] LHCb Collaboration, Aaij R, et al. Observation of associated production of a Z boson with a D meson in the forward region. J High Energy Phys 2014;04:091.
[61] LHCb Collaboration, Aaij R, et al. Production of associated and open charm hadrons in collisions at $\sqrt{s}=7$ and 8 TeV via double parton scattering. J High Energy Phys 2016;07:052.
[62] Axial Field Spectrometer Collaboration, Akesson T, et al. Double parton scattering in pp collisions at $\sqrt{s}=63$ GeV. Z Phys C 1987;34:163.
[63] CDF Collaboration, Abe F, et al. Study of four jet events and evidence for double parton interactions in $p\bar{p}$ collisions at $\sqrt{s}=1.8$ TeV. Phys Rev D 1993;47:4857.
[64] CDF Collaboration, Abe F, et al. Measurement of double parton scattering in $\bar{p}p$ collisions at $\sqrt{s}=1.8$ TeV. Phys Rev Lett 1997;79:584.
[65] D0 Collaboration, Abazov VM, et al. Double parton interactions in $\gamma+3$ jet events in $p\bar{p}$ collisions at $\sqrt{s}=1.96$ TeV. Phys Rev D 2010;81:052012.
[66] D0 Collaboration, Abazov VM, et al. Double parton interactions in $\gamma+3$ jet and $\gamma+b/c$ jet $+2$ jet events in $p\bar{p}$ collisions at $\sqrt{s}=1.96$ TeV. Phys Rev D 2014;89:072006.

[67] D0 Collaboration, Abazov VM, et al. Study of double parton interactions in diphoton + dijet events in $p\bar{p}$ collisions at $\sqrt{s} = 1.96$ TeV. Phys Rev D 2016;93:052008.
[68] UA2 Collaboration, Alitti J, et al. A study of multi-jet events at the CERN $\bar{p}p$ collider and a search for double parton scattering. Phys Lett B 1991;268:145.
[69] LHCb Collaboration, Aaij R, et al. Observation of J/ψ-pair production in collisions at $\sqrt{s} = 7$ TeV. Phys Lett B 2012;707:52.
[70] LHCb Collaboration, Aaij R, et al. Measurement of the J/ψ pair production cross-section in collisions at $\sqrt{s}$ = 13 TeV. J High Energy Phys 2017;06:047. Erratum ibid. 2017;10:068.
[71] LHCb collaboration, Alves AA Jr, et al. The LHCb detector at the LHC. JINST 2008;3:S08005.
[72] LHCb collaboration, Aaij R, et al. LHCb detector performance. Int J Mod Phys A 2015;30:1530022.
[73] LHCb Collaboration, Aaij R, et al. Measurement of b-hadron masses. Phys Lett B 2012;708:241.
[74] Sjöstrand T, Mrenna S, Skands P. A brief introduction to PYTHIA 8.1. Comput Phys Commun 2008;178:852.
[75] Belyaev I, Brambach T, Brook NH, et al. Handling of the generation of primary events in Gauss, the LHCb simulation framework. J Phys Conf Ser 2011;331:032047.
[76] Lange DJ. The EvtGen particle decay simulation package. Nucl Instrum Meth 2001;A462:152.
[77] Golonka P, Was Z. PHOTOS Monte Carlo: a precision tool for QED corrections in Z and W decays. Eur Phys J C 2006;45:97.
[78] Geant4 Collaboration, Allison J, et al. Geant4 developments and applications. IEEE Trans Nucl Sci 2006;53:270.
[79] Clemencic M, Corti G, Easo S, et al. The LHCb simulation application, Gauss: design, evolution and experience. J Phys Conf Ser 2011;331:032023.
[80] Hulsbergen WD. Decay chain fitting with a Kalman filter. Nucl Instrum Meth 2005;A552:566.
[81] Skwarnicki T. A study of the radiative cascade transitions between the Upsilon-prime and Upsilon resonances (Ph.D. thesis). Institute of Nuclear Physics: Krakow; 1986. DESY-F31-86-02 .
[82] LHCb Collaboration, Aaij R, et al. Measurement of J/ψ production in collisions at $\sqrt{s}$ = 7 TeV. Eur Phys J C 2011;71:1645.
[83] LHCb Collaboration, Aaij R, et al. Production of J/ψ and mesons in collisions at $\sqrt{s}$ = 8 TeV. J High Energy Phys 2013;06:064.
[84] LHCb Collaboration, Aaij R, et al. Measurement of forward J/ψ production cross-sections in collisions at $\sqrt{s}$ = 13 TeV. J High Energy Phys 2015;10:172. Erratum ibid. 2017;05:063.
[85] Particle Data Group, Tanabashi M, et al. Review of particle physics. Phys Rev D 2018;98:030001.
[86] Pivk M, Le Diberder FR. sPlot: a statistical tool to unfold data distributions. Nucl Instrum Meth 2005;A555:356.
[87] Xie Y. sFit: a method for background subtraction in maximum likelihood fit. arXiv:0905.0724, 2009.
[88] Braaten E, He L-P, Ingles K, et al. Charm-meson triangle singularity in e^+e^- annihilation into $D^{*0}\bar{D}^0 + \gamma$. Phys Rev D 2020;101:096020.
[89] Liu X-H, Wang Q, Zhao Q. Understanding the newly observed heavy pentaquark candidates. Phys Lett B 2016;757:231.
[90] Xie J-J, Geng L-S, Oset E. $f_2(1810)$ as a triangle singularity. Phys Rev D 2017;95:034004.
[91] Guo F-K, Hanhart C, Kalashnikova YS, et al. Interplay of quark and meson degrees of freedom in near-threshold states: a practical parametrization for line shapes. Phys Rev D 2016;93:074031.
[92] Langenbruch C. Parameter uncertainties in weighted unbinned maximum likelihood fits. arXiv:1911.01303, 2019.
[93] Cowan G, Cranmer K, Gross E, et al. Asymptotic formulae for likelihood-based tests of new physics. Eur Phys J C 2011;71:1554. Erratum ibid. C 2013;73:2501.

The LHCb experiment

LHCb is one of the four big experiments located on the most powerful particle accelerator in the world, the Larger Hadron Collider (LHC) at CERN. The LHCb detector includes a high-precision tracking system, particle identification detectors, electromagnetic and hadronic calorimeters and muon detectors, that record particles produced in proton-proton or heavy-ion collisions with a center-of-mass energy up to 13 TeV. The LHCb experiment aims at studies of flavor physics and QCD through precision measurements of particles containing charm or beauty quarks, in order to answer fundamental questions in particle physics, for example the origin of the asymmetry between matter and anti-matter and how does the strong interaction behaves at both high and low energies. The LHCb collaboration consists of more than 1400 members from 19 countries in 6 continents, including both physicists and engineers.

LHCb collaboration

R. Aaij[31], C. Abellán Beteta[49], T. Ackernley[59], B. Adeva[45], M. Adinolfi[53], H. Afsharnia[9], C.A. Aidala[82], S. Aiola[25], Z. Ajaltouni[9], S. Akar[64], J. Albrecht[14], F. Alessio[47], M. Alexander[58], A. Alfonso Albero[44], Z. Aliouche[61], G. Alkhazov[37], P. Alvarez Cartelle[47], A.A. Alves Jr[45], S. Amato[2], Y. Amhis[11], L. An[21], L. Anderlini[21], G. Andreassi[48], A. Andreianov[37], M. Andreotti[20], F. Archilli[16], A. Artamonov[43], M. Artuso[67], K. Arzymatov[41], E. Aslanides[10], M. Atzeni[49], B. Audurier[11], S. Bachmann[16], M. Bachmayer[48], J.J. Back[55], S. Baker[60], P. Baladron Rodriguez[45], V. Balagura[11, b], W. Baldini[20], J. Baptista Leite[1], R.J. Barlow[61], S. Barsuk[11], W. Barter[60], M. Bartolini[23, 47, h], F. Baryshnikov[79], J.M. Basels[13], G. Bassi[28], V. Batozskaya[35], B. Batsukh[67], A. Battig[14], A. Bay[48], M. Becker[14], F. Bedeschi[28], I. Bediaga[1], A. Beiter[67], V. Belavin[41], S. Belin[26], V. Bellee[48], K. Belous[43], I. Belyaev[38], G. Bencivenni[22], E. Ben-Haim[12], A. Berezhnoy[39], R. Bernet[49], D. Berninghoff[16], H.C. Bernstein[67], C. Bertella[47], E. Bertholet[12], A. Bertolin[27], C. Betancourt[49], F. Betti[19, e], M.O. Bettler[54], Ia. Bezshyiko[49], S. Bhasin[53], J. Bhom[33], L. Bian[72], M.S. Bieker[14], S. Bifani[52], P. Billoir[12], M. Birch[60], F.C.R. Bishop[54], A. Bizzeti[21, t], M. Bjørn[62], M.P. Blago[47], T. Blake[55], F. Blanc[48], S. Blusk[67], D. Bobulska[58], V. Bocci[30], J.A. Boelhauve[14], O. Boente Garcia[45], T. Boettcher[63], A. Boldyrev[80], A. Bondar[42, w], N. Bondar[37, 47], S. Borghi[61], M. Borisyak[41], M. Borsato[16], J.T. Borsuk[33], S.A. Bouchiba[48], T.J.V. Bowcock[59], A. Boyer[47], C. Bozzi[20], M.J. Bradley[60], S. Braun[65], A. Brea Rodriguez[45], M. Brodski[47], J. Brodzicka[33], A. Brossa Gonzalo[55], D. Brundu[26], E. Buchanan[53], A. Buonaura[49], C. Burr[47], A. Bursche[26], A. Butkevich[40], J.S. Butter[31], J. Buytaert[47], W. Byczynski[47], S. Cadeddu[26], H. Cai[72], R. Calabrese[20, g], L. Calero Diaz[22], S. Cali[22], R. Calladine[52], M. Calvi[24, i], M. Calvo Gomez[44, l], P. Camargo Magalhaes[53], A. Camboni[44], P. Campana[22], D.H. Campora Perez[47], A.F. Campoverde Quezada[5], S. Capelli[24, i], L. Capriotti[19, e], A. Carbone[19, e], G. Carboni[29], R. Cardinale[23, h], A. Cardini[26], I. Carli[6], P. Carniti[24, i], K. Carvalho Akiba[31], A. Casais Vidal[45], G. Casse[59], M. Cattaneo[47], G. Cavallero[47], S. Celani[48], R. Cenci[28], J. Cerasoli[10], A.J. Chadwick[59], M.G. Chapman[53], M. Charles[12], Ph. Charpentier[47], G. Chatzikonstantinidis[52], M. Chefdeville[8], C. Chen[3], S. Chen[26], A. Chernov[33], S.-G. Chitic[47], V. Chobanova[45], S. Cholak[48], M. Chrzaszcz[33], A. Chubykin[37], V. Chulikov[37], P. Ciambrone[22], M.F. Cicala[55], X. Cid Vidal[45], G. Ciezarek[47], F. Cindolo[19], P.E.L. Clarke[57], M. Clemencic[47], H.V. Cliff[54], J. Closier[47], J.L. Cobbledick[61], V. Coco[47], J.A.B. Coelho[11], J. Cogan[10], E. Cogneras[9], L. Cojocariu[36], P. Collins[47], T. Colombo[47], A. Contu[26], N. Cooke[52], G. Coombs[58], S. Coquereau[44], G. Corti[47], C.M. Costa Sobral[55], B. Couturier[47], D.C. Craik[63], J. Crkovská[66], M. Cruz Torres[1, y], R. Currie[57], C.L. Da Silva[66], E. Dall'Occo[14], J. Dalseno[45], C. D'Ambrosio[47], A. Danilina[38], P. d'Argent[47], A. Davis[61], O. De Aguiar Francisco[47], K. De Bruyn[47], S. De Capua[61], M. De Cian[48], J.M. De Miranda[1], L. De Paula[2], M. De Serio[18, d], D. De Simone[49], P. De Simone[22], J.A. de Vries[77], C.T. Dean[66], W. Dean[82], D. Decamp[8], L. Del Buono[12], B. Delaney[54], H.-P. Dembinski[14], A. Dendek[34], X. Denis[72], V. Denysenko[49], D. Derkach[80], O. Deschamps[9], F. Desse[11], F. Dettori[26, f], B. Dey[7], A. Di Canto[47], P. Di Nezza[22], S. Didenko[79], H. Dijkstra[47], V. Dobishuk[51], A.M. Donohoe[17], F. Dordei[26], M. Dorigo[28, x], A.C. dos Reis[1], L. Douglas[58], A. Dovbnya[50], A.G. Downes[8], K. Dreimanis[59], M.W. Dudek[33], L. Dufour[47], P. Durante[47], J.M. Durham[66], D. Dutta[61], M. Dziewiecki[16], A. Dziurda[33], A. Dzyuba[37], S. Easo[56], U. Egede[69], V. Egorychev[38], S. Eidelman[42, w], S. Eisenhardt[57], S. Ek-In[48], L. Eklund[58], S. Ely[67], A. Ene[36], E. Epple[66], S. Escher[13], J. Eschle[49], S. Esen[31], T. Evans[47], A. Falabella[19], J. Fan[3], Y. Fan[5], B. Fang[72], N. Farley[52], S. Farry[59], D. Fazz-

ini[11], P. Fedin[38], M. Féo[47], P. Fernandez Declara[47], A. Fernandez Prieto[45], F. Ferrari[19, e], L. Ferreira Lopes[48], F. Ferreira Rodrigues[2], S. Ferreres Sole[31], M. Ferrillo[49], M. Ferro-Luzzi[47], S. Filippov[40], R.A. Fini[18], M. Fiorini[20, g], M. Firlej[34], K.M. Fischer[62], C. Fitzpatrick[61], T. Fiutowski[34], F. Fleuret[11, b], M. Fontana[47], F. Fontanelli[23, h], R. Forty[47], V. Franco Lima[59], M. Franco Sevilla[65], M. Frank[47], E. Franzoso[20], G. Frau[16], C. Frei[47], D.A. Friday[58], J. Fu[25, p], Q. Fuehring[14], W. Funk[47], E. Gabriel[57], T. Gaintseva[41], A. Gallas Torreira[45], D. Galli[19, e], S. Gallorini[27], S. Gambetta[57], Y. Gan[3], M. Gandelman[2], P. Gandini[25], Y. Gao[4], M. Garau[26], L.M. Garcia Martin[46], P. Garcia Moreno[44], J. García Pardi nas[49], B. Garcia Plana[45], F.A. Garcia Rosales[11], L.Garrido[44], D. Gascon[44], C. Gaspar[47], R.E. Geertsema[31], D. Gerick[16], E. Gersabeck[61], M. Gersabeck[61], T. Gershon[55], D. Gerstel[10], Ph. Ghez[8], V. Gibson[54], A. Gioventù[45], P. Gironella Gironell[44], L. Giubega[36], C. Giugliano[20, g], K. Gizdov[57], V.V. Gligorov[12], C. Göbel[70], E. Golobardes[44, l], D. Golubkov[38], A. Golutvin[60, 79], A. Gomes[1, a], M. Goncerz[33], P. Gorbounov[38], I.V. Gorelov[39], C. Gotti[24, i], E. Govorkova[31], J.P. Grabowski[16], R. Graciani Diaz[44], T. Grammatico[12], L.A. Granado Cardoso[47], E. Graugés[44], E. Graverini[48], G. Graziani[21], A. Grecu[36], L.M. Greeven[31], P. Griffith[20, g], L. Grillo[61], L. Gruber[47], B.R. Gruberg Cazon[62], C. Gu[3], M. Guarise[20], P. A. Günther[16], E. Gushchin[40], A. Guth[13], Yu. Guz[43, 47], T. Gys[47], T. Hadavizadeh[69], G. Haefeli[48], C. Haen[47], S.C. Haines[54], P.M. Hamilton[65], Q. Han[7], X. Han[16], T.H. Hancock[62], S. Hansmann-Menzemer[16], N. Harnew[62], T. Harrison[59], R. Hart[31], C. Hasse[47], M. Hatch[47], J. He[5], M. Hecker[60], K. Heijhoff[31], K. Heinicke[14], A. M. Hennequin[47], K. Hennessy[59], L. Henry[25, 46], J. Heuel[13], A. Hicheur[68], D. Hill[62], M. Hilton[61], S.E. Hollitt[14], P.H. Hopchev[48], J. Hu[16], J. Hu[71], W. Hu[7], W. Huang[5], W. Hulsbergen[31], T. Humair[60], R.J. Hunter[55], M. Hushchyn[80], D. Hutchcroft[59], D. Hynds[31], P. Ibis[14], M. Idzik[34], D. Ilin[37], P. Ilten[52], A. Inglessi[37], K. Ivshin[37], R. Jacobsson[47], S. Jakobsen[47], E. Jans[31], B.K. Jashal[46], A. Jawahery[65], V. Jevtic[14], F. Jiang[3], M. John[62], D. Johnson[47], C.R. Jones[54], T.P. Jones[55], B. Jost[47], N. Jurik[62], S. Kandybei[50], Y. Kang[3], M. Karacson[47], J.M. Kariuki[53], N. Kazeev[80], M. Kecke[16], F. Keizer[54, 47], M. Kelsey[67], M. Kenzie[55], T. Ketel[32], B. Khanji[47], A. Kharisova[81], S. Kholodenko[43], K.E. Kim[67], T. Kirn[13], V.S. Kirsebom[48], O. Kitouni[63], S. Klaver[22], K. Klimaszewski[35], S. Koliiev[51], A. Kondybayeva[79], A. Konoplyannikov[38], P. Kopciewicz[34], R. Kopecna[16], P. Koppenburg[31], M. Korolev[39], I. Kostiuk[31, 51], O. Kot[51], S. Kotriakhova[37], P. Kravchenko[37], L. Kravchuk[40], R.D. Krawczyk[47], M. Kreps[55], F. Kress[60], S. Kretzschmar[13], P. Krokovny[42, w], W. Krupa[34], W. Krzemien[35], W. Kucewicz[83, 33, k], M. Kucharczyk[33], V. Kudryavtsev[42, w], H.S. Kuindersma[31], G.J. Kunde[66], T. Kvaratskheliya[38], D. Lacarrere[47], G. Lafferty[61], A. Lai[26], A. Lampis[26], D. Lancierini[49], J.J. Lane[61], R. Lane[53], G. Lanfranchi[22], C. Langenbruch[13], O. Lantwin[49, 79], T. Latham[55], F. Lazzari[28, u], R. Le Gac[10], S.H. Lee[82], R. Lefèvre[9], A. Leflat[39, 47], S. Legotin[79], O. Leroy[10], T. Lesiak[33], B. Leverington[16], H. Li[71], L. Li[62], P. Li[16], X. Li[66], Y. Li[6], Y. Li[6], Z. Li[67], X. Liang[67], T. Lin[60], R. Lindner[47], V. Lisovskyi[14], R. Litvinov[26], G. Liu[71], H. Liu[5], S. Liu[6], X. Liu[3], A. Loi[26], J. Lomba Castro[45], I. Longstaff[58], J.H. Lopes[2], G. Loustau[49], G.H. Lovell[54], Y. Lu[6], D. Lucchesi[27, n], S. Luchuk[40], M. Lucio Martinez[31], V. Lukashenko[31], Y. Luo[3], A. Lupato[61], E. Luppi[20, g], O. Lupton[55], A. Lusiani[28, s], X. Lyu[5], L. Ma[6], S. Maccolini[19, e], F. Machefert[11], F. Maciuc[36], V. Macko[48], P. Mackowiak[14], S. Maddrell-Mander[53], L.R. Madhan Mohan[53], O. Maev[37], A. Maevskiy[80], D. Maisuzenko[37], M.W. Majewski[34], S. Malde[62], B. Malecki[47], A. Malinin[78], T. Maltsev[42, w], H. Malygina[16], G. Manca[26, f], G. Mancinelli[10], R. Manera Escalero[44], D. Manuzzi[19, e], D. Marangotto[25, p], J. Maratas[9, v], J.F. Marchand[8], U. Marconi[19], S. Mariani[21, 47, z], C. Marin Benito[11], M. Marinangeli[48], P. Marino[48], J. Marks[16], P.J. Marshall[59], G. Martellotti[30], L. Martinazzoli[47], M. Martinelli[24, i], D. Martinez Santos[45], F. Martinez Vidal[46], A. Massafferri[1], M. Materok[13], R. Matev[47], A. Mathad[49], Z. Mathe[47], V. Matiunin[38], C. Matteuzzi[24], K.R. Mattioli[82], A. Mauri[49], E. Maurice[11, b], M. Mazurek[35], M. McCann[60], L. Mcconnell[17], T.H. Mcgrath[61], A. McNab[61], R. McNulty[17], J.V. Mead[59], B. Meadows[64], C. Meaux[10], G. Meier[14], N. Meinert[75], D. Melnychuk[35], S. Meloni[24, i], M. Merk[31, 77], A. Merli[25], L. Meyer Garcia[2], M. Mikhasenko[47], D.A. Milanes[73], E. Millard[55], M.-N. Minard[8], L. Minzoni[20, g], S.E. Mitchell[57], B. Mitreska[61], D.S. Mitzel[47], A. Mödden[14], R.A. Mohammed[62], R.D. Moise[60], T. Mombächer[14], I.A. Monroy[73], S. Monteil[9], M. Morandin[27], G. Morello[22], M.J. Morello[28, s], J. Moron[34], A.B. Morris[74], A.G. Morris[55], R. Mountain[67], H. Mu[3], F. Muheim[57], M. Mukherjee[7], M. Mulder[47], D. Müller[47], K. Müller[49], C.H. Murphy[62], D. Murray[61], P. Muzzetto[26], P. Naik[53], T. Nakada[48], R. Nandakumar[56], T. Nanut[48], I. Nasteva[2], M. Needham[57], I. Neri[20, g], N. Neri[25, p], S. Neubert[74], N. Neufeld[47], R. Newcombe[60], T.D. Nguyen[48], C. Nguyen-Mau[48, m], E.M. Niel[11], S. Nieswand[13], N. Nikitin[39], N.S. Nolte[47], C. Nunez[82], A. Oblakowska-Mucha[34], V. Obraztsov[43], S. Ogilvy[58], D.P. O'Hanlon[53], R. Oldeman[26, f], C.J.G. Onderwater[76], J. D.Osborn[82], A. Ossowska[33], J.M. Otalora Goicochea[2], T. Ovsiannikova[38], P. Owen[49], A. Oyanguren[46], B. Pagare[55], P.R. Pais[47], T. Pajero[28, 47, s], A. Palano[18], M. Palutan[22], Y. Pan[61], G. Panshin[81], A. Papanestis[56], M. Pappagallo[57], L.L. Pappalardo[20, g], C. Pappenheimer[64], W. Parker[65], C. Parkes[61], C.J. Parkinson[45], B. Passalacqua[20], G. Passaleva[21, 47], A. Pastore[18], M. Patel[60], C. Patrignani[19, e], A. Pearce[47], A. Pellegrino[31], M. Pepe Altarelli[47], S. Perazzini[19], D. Pereima[38], P. Perret[9], K. Petridis[53], A. Petrolini[23, h], A. Petrov[78], S. Petrucci[57], M. Petruzzo[25], A. Philippov[41], L. Pica[28], B. Pietrzyk[8], G. Pietrzyk[48], M. Pili[62], D. Pinci[30], J. Pinzino[47], F. Pisani[47], A. Piucci[16], V. Placinta[36], S. Playfer[57], J. Plews[52], M. Plo Casasus[45], F. Polci[12], M. Poli Lener[22], M. Poliakova[67], A. Poluektov[10], N. Polukhina[79, c], I. Polyakov[67], E. Polycarpo[2], G.J. Pomery[53], S. Ponce[47], A. Popov[43], D. Popov[5, 47], S. Popov[41], S. Poslavskii[43], K. Prasanth[33], L. Promberger[47], C. Prouve[45], V. Pugatch[51], A. Puig Navarro[49], H. Pullen[62], G. Punzi[28, o], R. Puthumanaillam Krishnankuttyelayath[10], W. Qian[5], J. Qin[5], R. Quagliani[12], B. Quintana[8], N.V. Raab[17], R.I. Rabadan Trejo[10], B. Rachwal[34], J.H. Rademacker[53], M. Rama[28], M. Ramos Pernas[45], M.S. Rangel[2], F. Ratnikov[41, 80], G. Raven[32], M. Reboud[8], F. Redi[48], F. Reiss[12], C. Remon Alepuz[46], Z. Ren[3], V. Renaudin[62], R. Ribatti[28], S. Ricciardi[56], D.S. Richards[56], K. Rinnert[59], P. Robbe[11], A. Robert[12], G. Robertson[57], A.B. Rodrigues[48], E. Rodrigues[59], J.A. Rodriguez Lopez[73], M. Roehrken[47], A. Rollings[62], V. Romanovskiy[43], M. Romero Lamas[45], A. Romero Vidal[45], J.D. Roth[82], M. Rotondo[22], M.S. Rudolph[67], T. Ruf[47], J. Ruiz Vidal[46], A. Ryzhikov[80], J. Ryzka[34], J.J. Saborido Silva[45], N. Sagidova[37], N. Sahoo[55], B. Saitta[26, f], C. Sanchez Gras[31], C. Sanchez Mayordomo[46], R. Santacesaria[30], C. Santamarina Rios[45], M. Santimaria[22], E. Santovetti[29, j], D. Saranin[79], G. Sarpis[61], M. Sarpis[74], A. Sarti[30], C. Satriano[30, r], A. Satta[29], M. Saur[5], D. Savrina[38, 39], H. Sazak[9], L.G. Scantlebury Smead[62], S. Schael[13], M. Schellenberg[14], M. Schiller[58], H. Schindler[47], M. Schmelling[15], T. Schmelzer[14], B. Schmidt[47], O. Schneider[48], A. Schopper[47], H.F. Schreiner[64], M. Schubiger[31], S. Schulte[48], M.H. Schune[11], R. Schwemmer[47], B. Sciascia[22], A. Sciubba[22], S. Sellam[68], A. Semennikov[38], A. Sergi[52, 47], N. Serra[49], J. Serrano[10], L. Sestini[27], A. Seuthe[14], P. Seyfert[47], D.M. Shangase[82], M. Shapkin[43], I. Shchemerov[79], L. Shchutska[48], T. Shears[59], L. Shekhtman[42, w], V. Shevchenko[78], E.B. Shields[24, i], E. Shmanin[79], J.D. Shupperd[67], B.G. Siddi[20], R. Silva Coutinho[49], L. Silva de Oliveira[2], G. Simi[27], S. Simone[18, d], I. Skiba[20, g], N. Skidmore[74], T. Skwarnicki[67], M.W. Slater[52], J.C. Smallwood[62], J.G. Smeaton[54], A. Smetkina[38], E. Smith[13], M. Smith[60], A. Snoch[31], M. Soares[19], L. Soares Lavra[9], M.D. Sokoloff[64], F.J.P. Soler[58], A. Solovev[37], I. Solovyev[37], F.L. Souza De Almeida[2], B. Souza De Paula[2], B. Spaan[14], E. Spadaro Norella[25, p], P. Spradlin[58], F. Stagni[47], M. Stahl[64], S. Stahl[47], P. Stefko[48], O. Steinkamp[49, 79], S. Stemmle[16], O. Stenyakin[43], H. Stevens[14], S. Stone[67], S. Stracka[28], M.E. Stramaglia[48], M. Straticiuc[36], D. Strekalina[79], S. Strokov[81], F. Suljik[62], J. Sun[26], L. Sun[72], Y. Sun[65], P. Svihra[61], P.N. Swallow[52], K. Swientek[34], A. Szabelski[35], T. Szumlak[34], M. Szymanski[47], S. Taneja[61], Z. Tang[3], T. Tekampe[14], F. Teubert[47], E. Thomas[47], K.A. Thomson[59], M.J. Tilley[60], V. Tisserand[9], S. T'Jampens[8], M. Tobin[6], S. Tolk[47], L. Tomassetti[20, g], D. Torres Machado[1], D.Y. Tou[12], M. Traill[58], M.T. Tran[48], E. Trifonova[79], C. Trippl[48], A. Tsaregorodtsev[10], G. Tuci[28, o], A. Tully[48], N. Tuning[31], A. Ukleja[35], D.J. Unverzagt[16], A. Usachov[31], A. Ustyuzhanin[41, 80], U. Uwer[16], A. Vagner[81], V. Vagnoni[19], A. Valassi[47], G. Valenti[19], M. van Beuzekom[31], H. Van Hecke[66], E. van Herwijnen[79], C.B. Van Hulse[17], M. van Veghel[76], R. Vazquez Gomez[45], P. Vazquez Regueiro[45], C. Vázquez Sierra[31], S. Vecchi[20], J.J. Velthuis[53], M. Veltri[21, q], A. Venkateswaran[67], M. Veronesi[31], M. Vesterinen[55], D. Vieira[64], M. Vieites Diaz[48], H. Viemann[75], X. Vilasis-Cardona[44], E. Vilella Figueras[59],

P. Vincent[12], G. Vitali[28], A. Vitkovskiy[31], A. Vollhardt[49], D. Vom Bruch[12], A. Vorobyev[37], V. Vorobyev[42, w], N. Voropaev[37], R. Waldi[75], J. Walsh[28], C. Wang[16], J. Wang[3], J. Wang[72], J. Wang[4], J. Wang[6], M. Wang[3], R. Wang[53], Y. Wang[7], Z. Wang[49], D.R. Ward[54], H.M. Wark[59], N.K. Watson[52], S.G. Weber[12], D. Websdale[60], C. Weisser[63], B.D.C. Westhenry[53], D.J. White[61], M. Whitehead[53], D. Wiedner[14], G. Wilkinson[62], M. Wilkinson[67], I. Williams[54], M. Williams[63, 69], M.R.J. Williams[61], F.F. Wilson[56], W. Wislicki[35], M. Witek[33], L. Witola[16], G. Wormser[11], S. A. Wotton[54], H. Wu[67], K. Wyllie[47], Z. Xiang[5], D. Xiao[7], Y. Xie[7], H. Xing[71], A. Xu[4], J. Xu[5], L. Xu[3], M. Xu[7], Q. Xu[5], Z. Xu[4], D. Yang[3], Y. Yang[5], Z. Yang[3], Z. Yang[65], Y. Yao[67], L.E. Yeomans[59], H. Yin[7], J. Yu[7], X. Yuan[67], O. Yushchenko[43], K.A. Zarebski[52], M. Zavertyaev[15, c], M. Zdybal[33], O. Zenaiev[47], M. Zeng[3], D. Zhang[7], L. Zhang[3], S. Zhang[4], Y. Zhang[47], A. Zhelezov[16], Y. Zheng[5], X. Zhou[5], Y. Zhou[5], X. Zhu[3], V. Zhukov[13, 39], J.B. Zonneveld[57], S. Zucchelli[19, e], D. Zuliani[27], G. Zunica[61].

[1]Centro Brasileiro de Pesquisas Físicas (CBPF), Rio de Janeiro, Brazil.
[2]Universidade Federal do Rio de Janeiro (UFRJ), Rio de Janeiro, Brazil.
[3]Center for High Energy Physics, Tsinghua University, Beijing, China.
[4]School of Physics State Key Laboratory of Nuclear Physics and Technology, Peking University, Beijing, China.
[5]University of Chinese Academy of Sciences, Beijing, China.
[6]Institute Of High Energy Physics (IHEP), Beijing, China.
[7]Institute of Particle Physics, Central China Normal University, Wuhan, Hubei, China.
[8]Univ. Grenoble Alpes, Univ. Savoie Mont Blanc, CNRS, IN2P3-LAPP, Annecy, France.
[9]Université Clermont Auvergne, CNRS/IN2P3, LPC, Clermont-Ferrand, France.
[10]Aix Marseille Univ, CNRS/IN2P3, CPPM, Marseille, France.
[11]Université Paris-Saclay, CNRS/IN2P3, IJCLab, Orsay, France.
[12]LPNHE, Sorbonne Université, Paris Diderot Sorbonne Paris Cité, CNRS/IN2P3, Paris, France.
[13]I. Physikalisches Institut, RWTH Aachen University, Aachen, Germany.
[14]Fakultät Physik, Technische Universität Dortmund, Dortmund, Germany.
[15]Max-Planck-Institut für Kernphysik (MPIK), Heidelberg, Germany.
[16]Physikalisches Institut, Ruprecht-Karls-Universität Heidelberg, Heidelberg, Germany.
[17]School of Physics, University College Dublin, Dublin, Ireland.
[18]INFN Sezione di Bari, Bari, Italy.
[19]INFN Sezione di Bologna, Bologna, Italy.
[20]INFN Sezione di Ferrara, Ferrara, Italy.
[21]INFN Sezione di Firenze, Firenze, Italy.
[22]INFN Laboratori Nazionali di Frascati, Frascati, Italy.
[23]INFN Sezione di Genova, Genova, Italy.
[24]INFN Sezione di Milano-Bicocca, Milano, Italy.
[25]INFN Sezione di Milano, Milano, Italy.
[26]INFN Sezione di Cagliari, Monserrato, Italy.
[27]Universita degli Studi di Padova, Universita e INFN, Padova, Padova, Italy.
[28]INFN Sezione di Pisa, Pisa, Italy.
[29]INFN Sezione di Roma Tor Vergata, Roma, Italy.
[30]INFN Sezione di Roma La Sapienza, Roma, Italy.
[31]Nikhef National Institute for Subatomic Physics, Amsterdam, Netherlands.
[32]Nikhef National Institute for Subatomic Physics and VU University Amsterdam, Amsterdam, Netherlands.
[33]Henryk Niewodniczanski Institute of Nuclear Physics Polish Academy of Sciences, Kraków, Poland.
[34]AGH – University of Science and Technology, Faculty of Physics and Applied Computer Science, Kraków, Poland.
[35]National Center for Nuclear Research (NCBJ), Warsaw, Poland.
[36]Horia Hulubei National Institute of Physics and Nuclear Engineering, Bucharest-Magurele, Romania.
[37]Petersburg Nuclear Physics Institute NRC Kurchatov Institute (PNPI NRC KI), Gatchina, Russia.
[38]Institute of Theoretical and Experimental Physics NRC Kurchatov Institute (ITEP NRC KI), Moscow, Russia, Moscow, Russia.
[39]Institute of Nuclear Physics, Moscow State University (SINP MSU), Moscow, Russia.
[40]Institute for Nuclear Research of the Russian Academy of Sciences (INR RAS), Moscow, Russia.
[41]Yandex School of Data Analysis, Moscow, Russia.
[42]Budker Institute of Nuclear Physics (SB RAS), Novosibirsk, Russia.
[43]Institute for High Energy Physics NRC Kurchatov Institute (IHEP NRC KI), Protvino, Russia, Protvino, Russia.
[44]ICCUB, Universitat de Barcelona, Barcelona, Spain.
[45]Instituto Galego de Física de Altas Enerxías (IGFAE), Universidade de Santiago de Compostela, Santiago de Compostela, Spain.
[46]Instituto de Fisica Corpuscular, Centro Mixto Universidad de Valencia – CSIC, Valencia, Spain.
[47]European Organization for Nuclear Research (CERN), Geneva, Switzerland.
[48]Institute of Physics, Ecole Polytechnique Fédérale de Lausanne (EPFL), Lausanne, Switzerland.
[49]Physik-Institut, Universität Zürich, Zürich, Switzerland.
[50]NSC Kharkiv Institute of Physics and Technology (NSC KIPT), Kharkiv, Ukraine.
[51]Institute for Nuclear Research of the National Academy of Sciences (KINR), Kyiv, Ukraine.
[52]University of Birmingham, Birmingham, United Kingdom.
[53]H.H. Wills Physics Laboratory, University of Bristol, Bristol, United Kingdom.

[54]Cavendish Laboratory, University of Cambridge, Cambridge, United Kingdom.
[55]Department of Physics, University of Warwick, Coventry, United Kingdom.
[56]STFC Rutherford Appleton Laboratory, Didcot, United Kingdom.
[57]School of Physics and Astronomy, University of Edinburgh, Edinburgh, United Kingdom.
[58]School of Physics and Astronomy, University of Glasgow, Glasgow, United Kingdom.
[59]Oliver Lodge Laboratory, University of Liverpool, Liverpool, United Kingdom.
[60]Imperial College London, London, United Kingdom.
[61]Department of Physics and Astronomy, University of Manchester, Manchester, United Kingdom.
[62]Department of Physics, University of Oxford, Oxford, United Kingdom.
[63]Massachusetts Institute of Technology, Cambridge, MA, United States.
[64]University of Cincinnati, Cincinnati, OH, United States.
[65]University of Maryland, College Park, MD, United States.
[66]Los Alamos National Laboratory (LANL), Los Alamos, United States.
[67]Syracuse University, Syracuse, NY, United States.
[68]Laboratory of Mathematical and Subatomic Physics, Constantine, Algeria, associated to [2].
[69]School of Physics and Astronomy, Monash University, Melbourne, Australia, associated to [55].
[70]Pontifícia Universidade Católica do Rio de Janeiro (PUC-Rio), Rio de Janeiro, Brazil, associated to [2].
[71]Guangdong Provencial Key Laboratory of Nuclear Science, Institute of Quantum Matter, South China Normal University, Guangzhou, China, associated to [3].
[72]School of Physics and Technology, Wuhan University, Wuhan, China, associated to [3].
[73]Departamento de Fisica, Universidad Nacional de Colombia, Bogota, Colombia, associated to [12].
[74]Universität Bonn – Helmholtz-Institut für Strahlen und Kernphysik, Bonn, Germany, associated to [16].
[75]Institut für Physik, Universität Rostock, Rostock, Germany, associated to [16].
[76]Van Swinderen Institute, University of Groningen, Groningen, Netherlands, associated to [31].
[77]Universiteit Maastricht, Maastricht, Netherlands, associated to [31].
[78]National Research Centre Kurchatov Institute, Moscow, Russia, associated to [38].
[79]National University of Science and Technology "MISIS", Moscow, Russia, associated to [38].
[80]National Research University Higher School of Economics, Moscow, Russia, associated to [41].
[81]National Research Tomsk Polytechnic University, Tomsk, Russia, associated to [38].
[82]University of Michigan, Ann Arbor, United States, associated to [67].
[83]AGH – University of Science and Technology, Faculty of Computer Science, Electronics and Telecommunications, Kraków, Poland.
[a]Universidade Federal do Triângulo Mineiro (UFTM), Uberaba-MG, Brazil.
[b]Laboratoire Leprince-Ringuet, Palaiseau, France.
[c]P.N. Lebedev Physical Institute, Russian Academy of Science (LPI RAS), Moscow, Russia.
[d]Università di Bari, Bari, Italy.
[e]Università di Bologna, Bologna, Italy.
[f]Università di Cagliari, Cagliari, Italy.
[g]Università di Ferrara, Ferrara, Italy.
[h]Università di Genova, Genova, Italy.
[i]Università di Milano Bicocca, Milano, Italy.
[j]Università di Roma Tor Vergata, Roma, Italy.
[k]AGH – University of Science and Technology, Faculty of Computer Science, Electronics and Telecommunications, Kraków, Poland.
[l]DS4DS, La Salle, Universitat Ramon Llull, Barcelona, Spain.
[m]Hanoi University of Science, Hanoi, Vietnam.
[n]Università di Padova, Padova, Italy.
[o]Università di Pisa, Pisa, Italy.
[p]Università degli Studi di Milano, Milano, Italy.
[q]Università di Urbino, Urbino, Italy.
[r]Università della Basilicata, Potenza, Italy.
[s]Scuola Normale Superiore, Pisa, Italy.
[t]Università di Modena e Reggio Emilia, Modena, Italy.
[u]Università di Siena, Siena, Italy.
[v]MSU – Iligan Institute of Technology (MSU-IIT), Iligan, Philippines.
[w]Novosibirsk State University, Novosibirsk, Russia.
[x]INFN Sezione di Trieste, Trieste, Italy.
[y]Universidad Nacional Autonoma de Honduras, Tegucigalpa, Honduras.
[z]Università di Firenze, Firenze, Italy.